molecular pharmaceutics

Article

pubs.acs.org/molecularpharmaceutics

# Enhancement of the Targeting Capabilities of the Paclitaxel-Loaded Pluronic Nanoparticles with a Glycol Chitosan/Heparin Composite

Soon Hong Yuk,*[,†] Keun Sang Oh,[‡] Sun Hang Cho,[§] Sang Yoon Kim,[∥] Sangkwon Oh,[⊥] Jin Ho Lee,[⊥] Kwangmeyung Kim,[‡] and Ick Chan Kwon[‡]

[†]College of Pharmacy, Korea University, Jochiwon, Yeongi, Chungnam, 339-700, Republic of Korea

[‡]Biomedical Research Center, Korea Institute of Science and Technology, 39-1 Hawolgok-dong, Seongbuk-gu, Seoul 136-791, Republic of Korea

[§]Nanobiomaterials Laboratories, Korea Research Institute of Chemical Technology, P.O. Box 107, Yusung, Daejeon 305-600, Republic of Korea

[∥]Department of Otolaryngology, Asan Medical Center, University of Ulsan, College of Medicine, 388-1 Pungnap-dong, Songpa-gu, Seoul 138-736, Republic of Korea

[⊥]Department of Advanced Materials, Hannam University, 461-6 Jeonmin-dong, Yusung-gu, Daejeon 305-811, Republic of Korea

Supporting Information

**ABSTRACT:** An enhancement of tumor-targeting capability was demonstrated with paclitaxel (PTX)-loaded Pluronic nanoparticles (NPs) with immobilized glycol chitosan and heparin. The PTX-loaded Pluronic NPs were prepared as described in our previous report by means of a temperature-induced phase transition in a mixture of Pluronic F-68 and liquid polyethylene glycol (PEG; molecular weight: 400) containing PTX. The liquid PEG is used as the solubilizer of PTX, and Pluronic F-68 is the polymer that encapsulates the PTX. The glycol chitosan and heparin were immobilized on the surface of the Pluronic NPs in an aqueous medium, and a powdery form of the glycol chitosan/heparin immobilized Pluronic NPs (composite NPs) was obtained by freeze-drying. Field emission scanning electron microscopy and a particle size analyzer were used to observe the morphology and size distribution of the prepared NPs. To apply the composite NPs as a delivery system for the model anticancer drug PTX, the release pattern and pharmacokinetic parameters were observed, and the tumor growth was monitored by injecting the composite NPs into the tail veins of tumor-bearing mice. An enhancement of tumor-targeting capability of NPs was verified by using noninvasive live animal imaging technology to observe the time-dependent excretion profile, the in vivo biodistribution, circulation time, and the tumor-targeting capability of composite NPs.

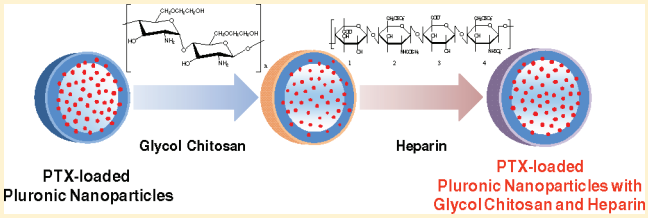


**KEYWORDS:** *glycol chitosan/heparin composite, Pluronic nanoparticles, paclitaxel, enhancement of tumor-targeting capability, cancer therapy*

## 1. INTRODUCTION

Considerable progress has been made in understanding how nanoparticles (NPs) can be used for cancer therapeutics; they are being introduced in an attempt to overcome several limitations of conventional chemotherapeutics.[1−3] Properly designed NPs can accumulate in tumors, by either passive or active targeting, without being eliminated from the body.[4,5] Passive targeting of NPs to tumors is expected based on the enhanced permeability and retention (EPR) effect.[6,7] However, the EPR effect is not a constant feature of tumor vessels,[8] and an attractive alternative would be to use NPs to target specific molecular receptors in the tumor cells.[9] For the specific targeting to tumor cells through the molecular recognition of unique cancer-specific markers, targeting ligands were chemically conjugated to the NPs containing therapeutics.[10−13] However, the efficiency of targeting tumor cells is generally low.

In a previous study, we focused on the specific interactions between a tumor and a glycol chitosan/heparin composite.[14] To observe the interaction, we used magnetic resonance (MR) imaging with glycol chitosan/heparin immobilized iron oxide NPs as a MR imaging probe. We also reported that the antitumor efficacy was enhanced by the use of paclitaxel (PTX)-loaded Pluronic NPs on account of the EPR effect.[15] The liquid PEG (molecular weight: 400) is used as a solubilizer of PTX and the polymer that encapsulates the PTX is composed of Pluronics (poly(ethylene oxide)−poly(propylene oxide)−poly(ethylene oxide) triblock copolymer, F-68). The stirring of the liquid polymer mixture formed emulsions composed of PEG containing PTX and liquidized Pluronic F-68 above transition temperature, and the melted mixture was subsequently solidified to form PTX-loaded Pluronic NPs.

**Received:** June 1, 2011
**Revised:** December 5, 2011
**Accepted:** December 12, 2011
**Published:** December 13, 2011





dx.doi.org/10.1021/mp200278s | *Mol. Pharmaceutics* 2012, 9, 230−236

These polymeric NPs have an increased circulation time in the body and, because of the EPR effect, are believed to accumulate in tumors.

This study demonstrates that PTX-loaded Pluronic NPs with immobilized glycol chitosan and heparin (composite NPs) have enhanced tumor-targeting capabilities. Glycol chitosan is emerging as a novel drug carrier because of its solubility and in vivo biocompatibility.[16] It also has the targeting characteristics based on the EPR effect.[17] Heparin, which is best known for its anticoagulant properties, is a highly sulfated, anionic polysaccharide composed of repeating glucosamine and uronic acid residues.[18,19] The ionic interaction of cationic glycol chitosan and anionic heparin stabilizes the glycol chitosan/heparin composite on the surface of PTX-loaded Pluronic NPs. To apply the composite NPs as a delivery system for PTX, we evaluated the drug release pattern, pharmacokinetic parameters, therapeutic efficacy, and in vivo biodistribution. The results are confirmed in two ways: by applying near-infrared fluorescence (NIRF) imaging technology to tumor-bearing mice and by observing the increased antitumor efficacy of PTX-loaded Pluronic NPs with immobilized glycol chitosan and heparin.

## 2. EXPERIMENTAL SECTION

**2.1. Materials.** Pluronic F-68 (Pluronics, poly(ethylene oxide)−poly(propylene oxide)−poly(ethylene oxide) triblock copolymer ($M_w$ = 8350; (EO)79(PO)28(EO)79) was obtained from BASF Corp., Korea, and used as received. Poly(ethylene glycol) (PEG, molecular weight: 400) was purchased from CRODA (Yorkshire, UK). PTX (anhydrous form) was purchased from Samyang Genex Co. (Daejeon, Korea). Glycol chitosan (molecular weight: 250 000) was purchased from Sigma Co. (St. Louis, MO, USA). Heparin sodium (189 IU $mg^{-1}$, $M_w$: 12 500) was purchased from Celsus Laboratories (Cincinnati, OH, USA). The monoreactive hydroxysuccinimide ester of Cy5.5 (Cy5.5-NHS) was obtained from Amersham Bioscience (Piscataway, NJ, USA).

**2.2. Preparation of PTX-Loaded Pluronic NPs.** PTX-loaded Pluronic NPs were prepared by means of a temperature-induced phase transition. First, 200 mg of PEG and 78.9 mg of PTX (loading amount: 7.5 wt %) were mixed to form a drug-loaded phase, which was subsequently mixed with 800 mg of Pluronic F-68. As the temperature was increased to 120 °C, the mixture melted into a liquid phase. After the equilibrium was maintained at 120 °C for 90 min, the liquid mixture was then cooled to 0 °C for 10 min to induce a phase transition. To evaluate the physicochemical characteristics of PTX-loaded Pluronic NPs, we added a predetermined amount of distilled−deionized water or phosphate buffered solution (PBS, pH 7.4) to the dried sample and sonicated the sample for 1 min to produce well-dispersed NPs in each solution.

**2.3. Immobilization of Glycol Chitosan and Heparin on the Surface of PTX-Loaded Pluronic NPs.** For the immobilization of glycol chitosan and heparin on the surface of PTX-loaded Pluronic NPs, we added 20 mL of distilled−deionized water to 100 mg of the prepared Pluronic NPs and sonicated the mixture for 1 min to produce well-dispersed Pluronic NPs in an aqueous medium. We then added 0.5 mL of a 0.00125 wt % glycol chitosan solution to form glycol chitosan-adsorbed Pluronic NPs via hydrogen bonding. Next we stabilized the glycol chitosan that adhered to the Pluronic NPs by supplementing the colloidal solution with 0.5 mL of 0.0625 wt % heparin aqueous solution. Finally, the colloidal solution was freeze-dried to obtain a powdery form of composite NPs.

**2.4. Fourier Transform Infrared Measurements.** Fourier transform infrared (FT-IR) measurements were performed to observe the interaction of F-68 and glycol chitosan. For the measurement, we cast thin films composed of F-68 and glycol chitosan onto separate $CaF_2$ plate at room temperature; the films were cast from a 5 wt % F-68 aqueous solution containing glycol chitosan. Most of the water in the films was removed by evaporation at 40 °C in a vacuum oven for 48 h. FT-IR spectra of the dried film were taken on 1000 PC spectroscope (Perkin-Elmer, USA) with 64 average scans at a resolution of 4 $cm^{-1}$.

**2.5. Particle Size and Morphology of Composite NPs.** The particle size distribution, the zeta potential, and the stability of composite NPs (3 mg/mL of composite NPs dispersed in PBS) were measured with an electrophoretic light scattering device (ELS-8000, Otsuka Electronics, Japan) at 25 °C ± 0.1 °C. When the difference between the measured and the calculated baselines was less than 0.1 %, the correlation function was accepted. A nonlinear regularized inverse Laplacian transformation technique was used to obtain the distribution of the decay constant. The mean diameter was determined with the Stokes−Einstein equation. FE-SEM images were also taken to observe the morphology of composite NPs. For the FE-SEM measurement, 0.1 wt % aqueous solutions of the composite NPs were prepared in the distilled−deionized water. Each solution was dropped on a carbon mount and then dried at 25 °C in a vacuum oven for 24 h. FE-SEM images were taken with a JSM-6700F microscope operating at 5 kV.

**2.6. In Vitro Drug Release Characteristics of PTX-Loaded Composite NPs.** To measure the release pattern of PTX from the NPs, 10 mg of NPs was dispersed in 10 mL of PBS and put into a dialysis bag (MWCO: 12 000−14 000, Spectrum, Rancho Dominquez, CA), which was immersed in 100 mL of PBS, containing 0.1% (w/v) Tween 80. The experimental setup was placed in a shaking water bath maintained at 37 °C and shaken horizontally at 100 rpm. At predetermined time intervals, 2 mL of aliquots of release medium (PBS) were withdrawn, and the total release medium was replaced with 100 mL of fresh PBS to maintain the sink conditions. The quantification of released PTX was determined by reverse-phase high performance liquid chromatography (RP-HPLC) using a Capcell-pack $C_{18}$ column and an acetonitrile/water (60:40, v/v) mobile phase over 10 min at a flow rate of 1.2 mL/min. The eluent was monitored by UV absorption at 227 nm.

**2.7. In Vivo Biodistribution and Tumor-Targeting Capability of PTX-Loaded Pluronic NPs in Tumor-Bearing Mice.** For in vivo experiments, SCC-7 (squamous cell carcinoma) cells were induced in male C3H/HeN mice (5.5 weeks old, ORIENT BIO Inc., Korea) by means of a subcutaneous injection of $1.0 \times 10^6$ cells suspended in a cell culture medium (RPMI 1640, 10% fetal bovine serum, 1% antibiotic agent). When the tumor volume reached approximately 250 $mm^3$ to 300 $mm^3$, the mice received an intravenous injection of Cy5.5-/PTX-loaded NPs with 10 mg/kg of PTX. To measure the tissue distribution, the time-dependent excretion profile, and the tumor-targeting capability, we positioned the animal on an eXplore Optix system (Advanced Research Technologies Inc., Montreal, Canada). The mice under anesthetic state by the inhalation of Gerolan sol. (enflurane as the active agent, Choong Wae PHARMA Co.,

**Scheme 1. Immobilization of Glycol Chitosan and Heparin on the Surface of PTX-Loaded Pluronic NPs**

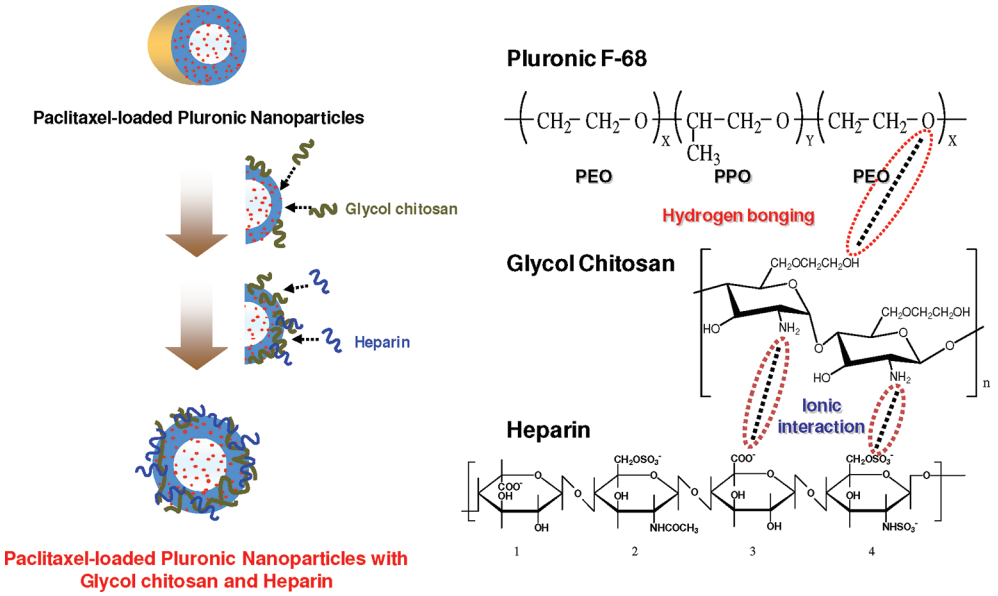


Korea) were automatically moved into the imaging chamber for scanning. Laser power was optimized at 6 $\mu$W, and the count time was set at 0.3 s per point. Excitation and emission spots were raster-scanned in 1 mm steps over the selected region of interest to generate emission wavelength scans. A 670 nm pulsed laser diode was used to excite the Cy5.5 molecules. A NIR fluorescence emission at 700 nm was collected and detected with the aid of a fast photomultiplier tube (Hammamatsu, Japan) and a time-correlated single photon counting system (Becker and Hickl GmbH, Berlin, Germany). The in vivo characteristics of Cy5.5-/PTX-loaded NPs were confirmed by measuring the NIR fluorescence intensity in the SCC-7 tumor-bearing mice ($n$ = 5). Data were calculated by using the region of interest (ROI) function of the Analysis Workstation software (Advanced Research Technologies). To compare tissue and tumor distributions of Cy5.5/PTX-loaded Pluronic NPs, the mice were sacrificed 3 days postinjection. The major organs including the liver, lung, spleen, kidney, and heart, as well as the tumor, were dissected from the mice, and their fluorescence intensities were determined by using a 12-bit CCD camera (Image Station 4000 MM; Kodak, New Haven, CT) equipped with a special C-mount lens and a Cy5.5 bandpass emission filter (680−720 nm; Omega Optical). Identical illumination settings (e.g., lamp voltage, filter, exposure time) were used in all animal imaging experiments. All animal experiments were carried out in accordance with the guidelines for animal experiments at the Korea Institute of Science and Technology, Republic of Korea.

**2.8. Pharmacokinetic Studies of PTX-Loaded NPs.** Healthy Sprague−Dawley rats (male, 7 weeks, 200 ± 20) were injected through the tail vein with 4 mg/kg of Taxol, Pluronic NPs, and the composite NPs. Blood samples (0.5 mL) were taken from the jugular vein at various times (0.08, 0.25, 0.5, 1, 1.5, 2, 4, 6, 8, and 24 h) and collected by retro-orbital plexus puncture into heparinized tubes. The samples were vortexed at the rate of 1000 rpm for 5 min and then centrifuged immediately (10,000 rpm, 5 min). Plasma samples were stored at −50 °C and subsequently analyzed by a LC/MS/MS system (3200 Q TRAP, Applied Biosystems, USA). Pharmacokinetic analysis was performed by using Phoenix WinNolin (Version 3.1, Pharsight Co., Mountainview, CA, USA). The maximum plasma concentration ($C_{max}$) and area under the plasma concentration−time profile from time zero to the time of the last quantifiable concentration ($AUC_{last}$) after infusion administration were observed values from the experimental data and were fitted to the noncompartment modeling (best fit).

**2.9. Antitumor Efficacy of PTX-Loaded NPs in Tumor-Bearing Mice.** Tumors were produced in C3H/HeN mice as described above. When the tumors grew to approximately 100−150 mm$^3$, the mice were divided into four groups: the first group was a control group treated with normal saline ($n$ = 5); the second group was treated with free PTX formulated in Tween 80 (PTX in the Cremophor EL formulation was 10 mg/kg) at 10 mg/kg ($n$ = 5); the third group was treated with PTX-loaded Pluronic NPs ($n$ = 5); the fourth group was treated with composite NPs at 10 mg PTX/kg ($n$ = 5). Each sample was injected every 3 days for 15 days.

**2.10. Statistical Analysis.** The data are expressed as the mean ± SEM of at least three experiments. The data for in vivo characteristics using the NIR fluorescence system were calculated by using the region of interest (ROI) function of the Analysis Workstation software (ART Advanced Research Technologies Inc., Montreal, Canada). The ORIGIN 7.0 statistical software program (OriginLab Corp., USA) was used for the data processing.

## 3. RESULTS

**3.1. Immobilization of Glycol Chitosan and Heparin on the Surface of PTX-Loaded Pluronic NPs.** The preparation of PTX-loaded Pluronic NPs is based on the preparation method in our previous report.[15] A mixture of PEG containing PTX and Pluronic F-68 was melted into a liquid phase at 120 °C for 90 min and cooled down to 0 °C to form PTX-loaded Pluronic NPs. The core/shell structure of the PTX-loaded Pluronic NPs was verified by means of a cryogenic TEM measurement. The spherical shape and size of 7.5 wt % PTX-loaded Pluronic NPs were confirmed by FE-SEM. Glycol chitosan and heparin were immobilized on the surface of PTX-loaded Pluronic NPs to obtain composite NPs (see Scheme 1).


dx.doi.org/10.1021/mp200278s | Mol. Pharmaceutics 2012, 9, 230−236

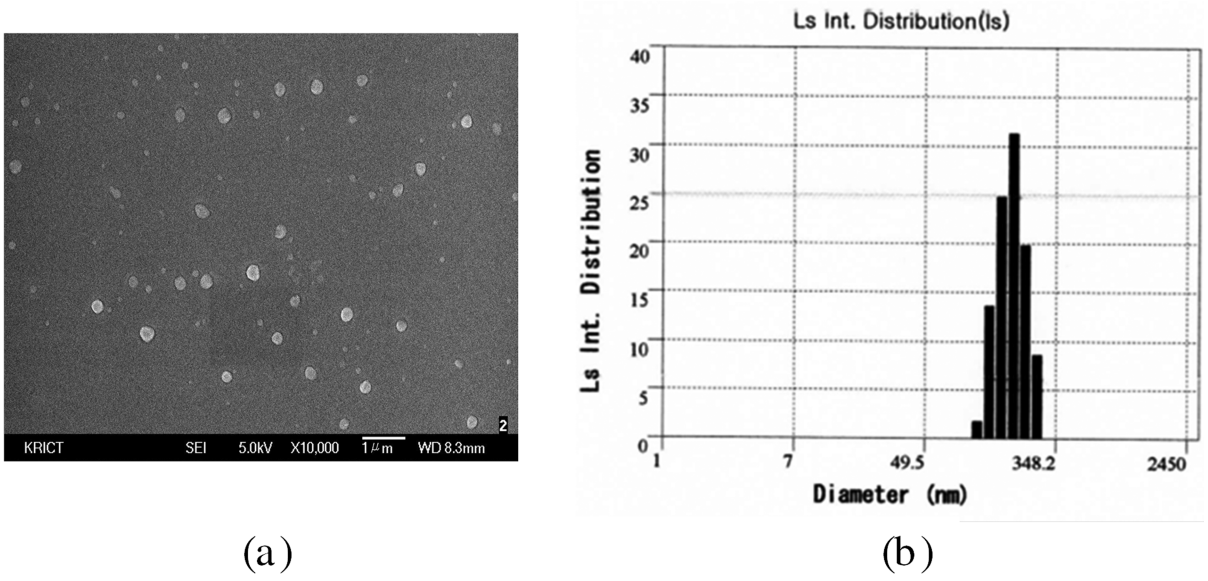


**Figure 1.** (a) FE-SEM image and (b) size distribution of composite NPs.

The FE-SEM image in Figure 1 was taken after glycol chitosan and heparin were immobilized on the surface of the PTX-loaded Pluronic NPs. Spherical NPs were formed with an average diameter of approximately 180 nm.

To verify the interaction of PTX-loaded Pluronic NPs with glycol chitosan, FT-IR spectra of a Pluronic F-68 and a Pluronic F-68/glycol chitosan mixture were observed. Pluronic F-68 has a hydroxyl group at the each end, and the absorption peak occurs at approximately 3500 $cm^{-1}$ as shown in Figure 2. When glycol chitosan is mixed with Pluronic F-68, the absorbance from the hydroxyl group of Pluronic F-68 is decreased.

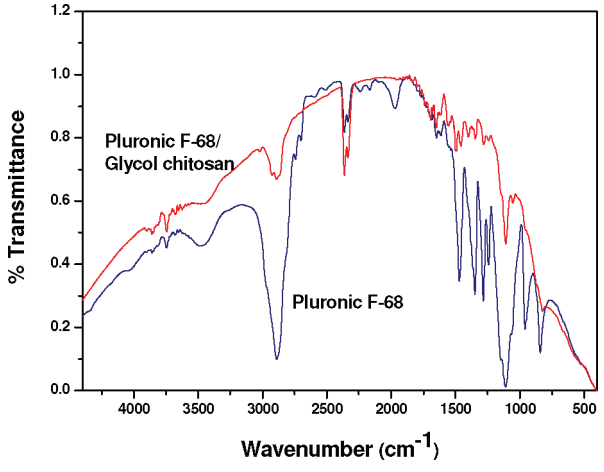


**Figure 2.** FT-IR spectra of a Pluronic and a Pluronic/glycol chitosan mixture.

**3.2. In Vitro Drug Release Characteristics of PTX-loaded Composite NPs.** As shown in Figure 3, we used a dialysis system to examine the in vitro release of PTX-loaded Pluronic NPs with and without glycol chitosan/heparin composite. A similar release pattern was observed, and approximately 30% of the loaded PTX was quickly released; this phase was followed by a sustained release for up to 48 h. The overall release rate of the composite NPs is lower than that of the Pluronic NPs.

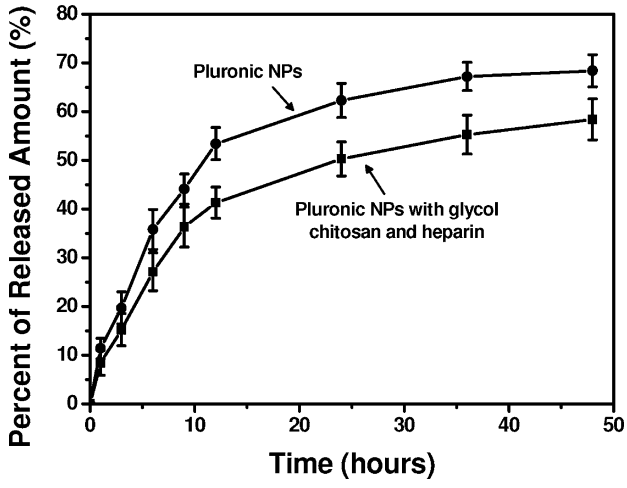


**Figure 3.** Release pattern of PTX from Pluronic NPs (loading amount: 7.50 ± 1.01 wt %) and composite NPs (loading amount: 7.41 ± 1.12 wt %).

**3.3. In Vivo Biodistribution, Pharmacokinetics, and Tumor-Targeting Capability of PTX-Loaded Pluronic NPs in Tumor-Bearing Mice.** After the mice with SCC-7 tumors were intravenously injected, we monitored the time-dependent biodistribution of the PTX-loaded Pluronic NPs and composite NPs (Figure 4). For the injection, the NPs were loaded with 0.1 wt % Cy5.5, a NIR (near-infrared) fluorescent dye. We then used an optical imaging system to monitor the dye in the live animals. Mice with Cy5.5/PTX-loaded composite NPs (10 mg/kg) reveal a strong NIR fluorescence signal in the tumor area within 1 h of injection; however, the situation is different for mice with Pluronic NPs (Figure 4a). We were able to distinguish tumors from the surrounding background tissue 1 h after the injection The NIR signal reached its maximum level 6 h after the injection, and the fluorescence continued for up to 48 h.

Furthermore, the fluorescence images in Figure 4b showed that 3 days after intravenous administration the fluorescence intensity was higher in tumors than in other major organs (such as the liver, lung, kidney, spleen, and heart), indicating that the


dx.doi.org/10.1021/mp200278s | Mol. Pharmaceutics 2012, 9, 230–236

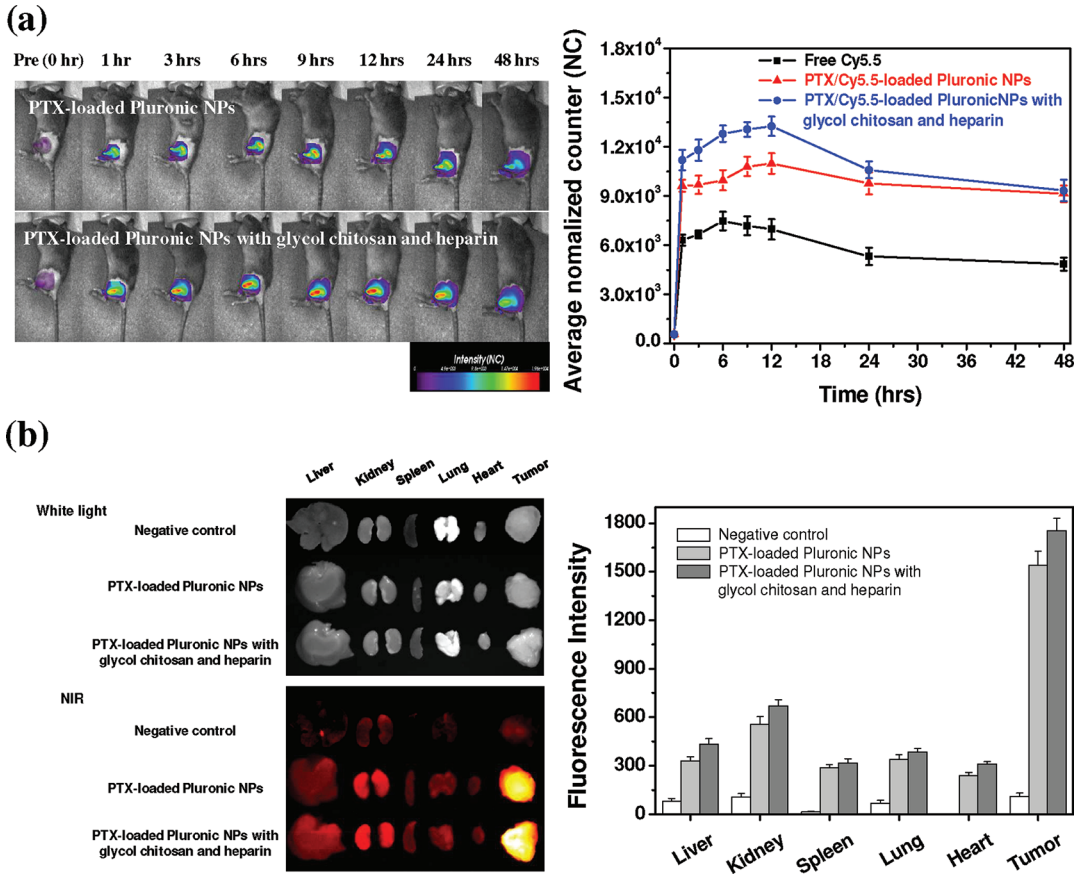


**Figure 4.** (a) In vivo noninvasive NIR images and quantification analysis of PTX/Cy5.5-loaded NPs and (b) representative ex vivo white light images and NIR images and quantification analysis of dissected organs of mice bearing SCC-7 cells sacrificed at 72 h.

EPR effect causes NPs to preferentially accumulate in tumor tissue. In addition, the NIR fluorescence total photon counts per gram of tumor tissue were 2.5−5 times higher than those of other organs. That means that the Cy5.5/PTX-loaded Pluronic NPs selectively target tumor tissues. Note also that fluorescence intensity is greater with the composite NPs than with Pluronic NPs.

To support the fact that the composite NPs are long-circulating, pharmacokinetic studies were performed (see Figure 5). After the administration of free PTX, PTX-loaded Pluronic NPs, and PTX-loaded Pluronic NPs with glycol chitosan and heparin (the composite NPs), the peak of plasma concentration ($C_{max}$) obtained was 121.6545 ± 11.6474 ng/mL, 188.0441 ± 51.3152 ng/mL, and 339.1482 ± 16.2986 ng/mL, respectively. The area under the plasma concentration−time profile from time zero to the time of the last quantifiable concentration ($AUC_{last}$) was 85.0047 ± 7.5987 ng·h/mL, 179.782 ± 13.5721 ng·h/mL, and 394.5316 ± 74.5345 ng·h/mL, respectively.

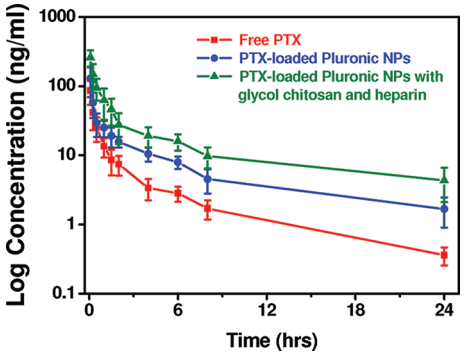


**Figure 5.** Mean plasma concentration−time profiles of PTX in Cremophor EL, PTX-loaded Pluronic NPs, and PTX-loaded Pluronic NPs with glycol chitosan and heparin (the composite NPs). Each data point represents the mean ± SEM of five animals.

**3.4. Antitumor Efficacy of PTX-Loaded NPs in Tumor-Bearing Mice.** We also examined how PTX-loaded Pluronic NPs with immobilized glycol chitosan and heparin change the tumor efficacy in vivo in SCC-7 tumor bearing mice (Figure 6). The mice were injected with PTX in a Cremophor EL formulation (10 mg/kg), Pluronic NPs, composite NPs, or saline (200 $\mu$L). The tumor size was similar for all treatments on day 5, at which time the animals received the second injection. By day 10, the increase in the tumor size was smaller in mice treated with composite NPs. This outcome confirms the enhanced tumor-targeting capability of composite NPs (Pluronic NPs with glycol chitosan and heparin). They are more effective than the other NPs at reducing the tumor volume.

## 4. DISCUSSION

Because the surface of the PTX-loaded Pluronic NPs is dominantly covered by Pluronic F-68, the immobilization of glycol chitosan on the surface of PTX-loaded Pluronic NPs is verified by observing the interaction between Pluronic F-68 and glycol chitosan. Pluronic F-68 has a hydroxyl group at the each


dx.doi.org/10.1021/mp200278s | Mol. Pharmaceutics 2012, 9, 230−236

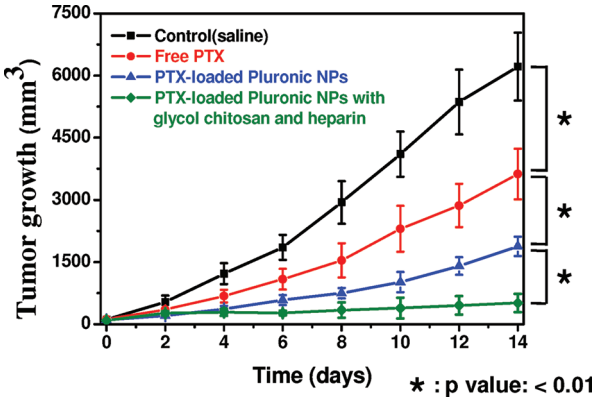


**Figure 6.** Therapeutic efficacy of PTX-loaded NPs on SCC-7 xenografts. Groups were intravenously given as saline, free PTX in Cremophor, Pluronic NPs, and Pluronic NPs with glycol chitosan and heparin after the SCC-7 tumor volume reached a range of 100−150 $mm^3$.

end, and the absorption peak occurs at approximately 3500 $cm^{-1}$ as shown in FT-IR spectra in Figure 3. When glycol chitosan is mixed with Pluronic F-68, the absorbance from the hydroxyl group of Pluronic F-68 is decreased due to the interaction of Pluronic F-68 and glycol chitosan via hydrogen bonding. The interaction of Pluronic F-68 and glycol chitosan forms the basis for the expected interaction of PTX-loaded Pluronic NPs and glycol chitosan.[20]

Because of the cationic characteristics of glycol chitosan-immobilized Pluronic NPs, anionic heparin can be introduced to the glycol chitosan-immobilized Pluronic NPs via an ionic interaction that forms composite NPs. The change of zeta potential was measured after glycol chitosan and heparin were immobilized on the surface of the PTX-loaded Pluronic NPs. The zeta potential after the immobilization of glycol chitosan on the surface of the PTX-loaded Pluronic NPs had a positive value of 14.46 mV. This value indicates that cationic glycol chitosan was immobilized onto Pluronic NPs. With the subsequent immobilization of heparin, the surface charge of the composite NPs acquired an anionic characteristic (−17.86 mV). Thus, an ionic interaction was efficiently induced.

The release rate of PTX from the NPs was decreased after the immobilization of glycol chitosan and heparin on the surface of PTX-loaded NPs. This is due to the presence of the glycol chitosan/heparin composite on the surface of the PTX-loaded Pluronic NPs. Because of hydrophilic characteristics of glycol chitosan/heparin composite, the release of hydrophobic PTX through glycol chitosan/heparin composite is controlled.

On the basis of these results, we confirm that glycol chitosan and heparin are immobilized onto the surface of PTX-loaded Pluronic NPs to form composite NPs.

To target tumors, NPs need a long half-life, and PEG can facilitate this requirement.[21,22] Because PTX-loaded Pluronic NPs were mainly composed of Pluronic F-68 and PEG is the major segment of Pluronic F-68, the Cy5.5/PTX-loaded Pluronic NPs selectively target tumor tissues. Note that the fluorescence intensity is greater with the composite NPs than with Pluronic NPs. This indicates that the glycol chitosan/heparin composite enhance the accumulation of NPs in tumors.

In the pharmacokinetic data as shown in Figure 5, NPs groups significantly altered the pharmacokinetic parameters of PTX compared to the control given free PTX. The composite NPs showed the highest values of $C_{max}$ and $AUC_{last}$. This is due to the long circulation of composite NPs, which leads to the enhancement of the targeting capabilities.

In previous work by Park et al.,[23] heparin-based NPs containing doxorubicin were prepared and characterized as a drug delivery vehicle for cancer therapy. Compared with free DOX, heparin-based NPs have a more enhanced ability to inhibit tumor growth. This ability is explained by the prolonged circulation of the heparin-based NPs, which in turn is attributed to the fact that heparin in the NPs reduces the opsonization by the reticuloendothelial system.

Studies on the tumor-associated activation of the coagulation cascade have shown that most solid tumors contain considerable amounts of fibrinogen-derived products.[24−26] In the treatment of solid tumors, heparin is ineffective at inhibiting the formation of fibrin at the tumor sites. Nevertheless heparin-immobilized NPs are expected to be localized at the tumor site. This expectation is based on the interactions of fibrinogen-derived products in the solid tumor and the heparin that is immobilized on composite NPs. The enhanced targeting capabilities of composite NPs can be explained in terms of these interactions.

In our previous report, we demonstrated that glycol chitosan/heparin composite enhanced the targeting characteristics of iron oxide NPs with immobilized glycol chitosan and heparin.[14] We also observed the improved antitumor efficacy with composite NPs. This outcome confirms that glycol chitosan/heparin composite plays an important role in enhancing the tumor-targeting capability of composite NPs.

## 5. CONCLUSIONS

Our results verify that the tumor-targeting capability of PTX-loaded Pluronic NPs can be enhanced with the immobilization of a glycol chitosan/heparin composite. FE-SEM and size distribution analyses show the formation of PTX-loaded Pluronic NPs with immobilized glycol chitosan and heparin (composite NPs). The eXplore Optix system reveals that Cy5.5 fluorescence from the composite NPs has an extended retention time at the tumor sites. The glycol chitosan/heparin immobilized on the Pluronic NPs may induce an interaction between the fibrinogen-derived products in the tumor tissue and the heparin on the composite NPs and thereby enhance the therapeutic efficacy. These preliminary results suggest that the targeting capability can be enhanced by the glycol chitosan/heparin composite, and this capability could be useful for designing a new type of drug carrier for improved antitumor activity.

## ■ ASSOCIATED CONTENT

### Ⓢ Supporting Information

Change of zeta potential after the immobilization of glycol chitosan and heparin on the surface of PTX-loaded Pluronic NPs. This material is available free of charge via the Internet at http://pubs.acs.org.

## ■ AUTHOR INFORMATION

### Corresponding Author

*Mailing address: Korea University, College of Pharmacy, Jochiwon, Yeongi, Chungnam, 339-700, Republic of Korea. Telephone: +82-41-860-1612. Fax: +82-41-860-1606. E-mail: shyuk@korea.ac.kr.

## ■ ACKNOWLEDGMENTS

This work was financially supported by the Korea Research Foundation (20110027932) and a grant from the fundamental R& D Program for Core Technology of Materials funded by the Ministry of Knowledge and Economy, Republic of Korea.

## ■ REFERENCES

(1) Milane, L.; Duan, Z.; Amiji, M. Development of EGFR-targeted polymer blend nanocarriers for combination paclitaxel/lonidamine delivery to treat multi-drug resistance in human breast and ovarian tumor cells. *Mol. Pharmaceutics* **2011**, *8*, 185−203.

(2) Hu, C. M.; Zhang, L. F. Therapeutic nanoparticles to combat cancer drug resistance. *Curr. Drug Metab.* **2009**, *10*, 836−84.

(3) Murakami, M.; Cabral, H.; Matsumoto, Y.; Wu, S.; Kano, M. R.; Yamori, T.; Nishiyama, N.; Kataoka, K. Improving drug potency and efficacy by nanocarrier-mediated subcellular targeting. *Sci. Transl. Med.* **2011**, *3*, 1−11.

(4) Ferrari, M. Cancer nanotechnology: opportunities and challenges. *Nat. Rev. Cancer* **2005**, *5*, 161−71.

(5) Davis, M. E.; Chen, Z.; Shin, D. M. Nanoparticle therapeutics: an emerging treatment modality for cancer. *Nat. Rev. Drug Discovery* **2008**, *7*, 771−82.

(6) Maeda, H.; Wu, J.; Sawa, T.; Matsumura, Y.; Hori, K. Tumor vascular permeability and the EPR effect in macromolecular therapeutics: a review. *J. Controlled Release* **2000**, *65*, 271−84.

(7) Lyer, A. K.; Khaled, G.; Fang, J.; Maeda, H. Exploiting the enhanced permeability and retention effect for tumor targeting. *Drug Discovery Today* **2006**, *11*, 812−8.

(8) Sinek, J.; Frieboes, H.; Zheng, X.; Cristini, V. Two-dimensional chemotherapy simulations demonstrate fundamental transport and tumor response limitations involving nanoparticles. *Biomed. Microdevices* **2004**, *6*, 297−309.

(9) Simberg, D.; Duza, T.; Park, J. H.; Essler, M.; Pilch, J.; Zhang, L.; Derfus, A. M.; Yang, M.; Hoffaman, R. M.; Bhatia, S.; Saiolor, M. J.; Ruoslahti, E. Biomimetic amplification of nanoparticle homing to tumors. *Proc. Natl. Acad. Sci. U.S.A.* **2007**, *104*, 932−6.

(10) Hoffman, J. A.; Giraudo, E.; Singh, M.; Zhang, L.; Inoue, M.; Porkka, K.; Hanahan, D.; Ruoslahti, E. Progressive vascular changes in a transgenic mouse model of squamous cell carcinoma. *Cancer Cell* **2003**, *4*, 383−91.

(11) Peer, D.; Karp, J. M.; Hong, S.; Farokhzad, O. C.; Margalit, R.; Langer, R. Nanocarriers as an emerging platform for cancer therapy. *Nat. Nanotechnol.* **2007**, *2*, 751−60.

(12) Lee, E. S.; Na, K.; Bae, Y. H. Super pH-sensitive multifunctional polymeric micelle. *Nano Lett.* **2005**, *5*, 325−9.

(13) Byrne, J. D.; Betancourt, T.; Brannon-Peppas, L. Active targeting schemes for nanoparticle systems in cancer therapeutics. *Adv. Drug Delivery Rev.* **2008**, *60*, 1615−26.

(14) Yuk, S. H.; Oh, K. S.; Cho, S. H.; Lee, B. S.; Kim, S. Y.; Kwak, B. K.; Kim, K.; Kwon, I. C. Glycol chitosan/heparin immobilized iron oxide nanoparticles with a tumor-targeting characteristic for magnetic resonance imaging. *Biomacromolecules* **2011**, *12*, 2335−43.

(15) Oh, K. S.; Song, J. Y.; Cho, S. H.; Lee, B. S.; Kim, S. Y.; Kim, K.; Jeon, H.; Kwon, I. C.; Yuk, S. H. Paclitaxel-loaded pluronic nanoparticles formed by a temperature-induced phase transition for cancer therapy. *J. Controlled Release* **2010**, *148*, 334−50.

(16) Kim, J. H.; Kim, Y. S.; Kim, S.; Park, J. H.; Kim, K.; Choi, K.; Chung, H.; Jeong, S. Y.; Park, R. W.; Kim, I. S.; Kwon, I. C. Hydrophobically modified glycol chitosan nanoparticles as carriers for paclitaxel. *J. Controlled Release* **2006**, *111*, 228−34.

(17) Park, K.; Kim, J. H.; Nam, Y. S.; Lee, S.; Nam, H. Y.; Kim, K.; Park, J. H.; Kim, I. S.; Choi, K.; Kim, S. Y.; Kwon, I. C. Effect of polymer molecular weight on the tumor targeting characteristics of self-assembled glycol chitosan nanoparticles. *J. Controlled Release* **2007**, *122*, 305−14.

(18) Qi, Y.; Zhao, G.; Liu, D.; Shriver, Z.; Sundaram, M.; Sengupta, S.; Venkataraman, G.; Langer, R.; Sasisekharan, R. Rational design of low-molecular weight heparins with improved in vivo activity. *Proc. Natl. Acad. Sci. U.S.A.* **2003**, *100*, 651−6.

(19) Kemp, M. M.; Linhart, R. J. Heparin-based nanoparticles. *WIREs Nanomed. Nanobiotechnol.* **2010**, *2*, 77−86.

(20) Oh, K. S.; Song, J. Y.; Yoon, S. J.; Park, Y.; Kim, D.; Yuk, S. H. Temperature-induced gel formation of core/shell nanoparticles for the regeneration of ischemic heart. *J. Controlled Release* **2010**, *146*, 207−11.

(21) Gabizon, A.; Shmeeda, H.; Horowitz, A. T.; Zalipsky, S. Tumor cell targeting of liposome-entrapped drugs with phospholipid-anchored folic acid-PEG conjugates. *Adv. Drug Delivery Rev.* **2004**, *56*, 1177−92.

(22) Ayen, W. Y.; Garkhal, K.; Kumar, N. Doxorubicin-loaded (PEG)3-PLA nanopolymersomes: effect of solvents and process parameters on formulation development and in vitro study. *Mol. Pharmaceutics* **2011**, *8*, 466−478.

(23) Park, K.; Lee, G. Y.; Kim, Y.-S.; Yu, M.; Park, R.-W.; Kim, I. S.; Kim, S. Y.; Byun, Y. Heparin-deoxycholic acid chemical conjugate as an anticancer drug carrier and its antitumor activity. *J. Controlled Release* **2006**, *114*, 300−6.

(24) Costantini, V.; Zacharski, L. R. Fibrin and cancer. *Thromb. Haemost.* **1993**, *69*, 406−14.

(25) Niers, T. M. H.; Klerk, C. P. W.; DiNisio, M.; Van Noorden, C. J. F.; Büller, H. R.; Reitsma, P. H.; Richel, D. J. Mechanisms of heparin induced anti-cancer activity in experimental cancer models. *Crit. Rev. Oncol. Hematol.* **2007**, *61*, 195−207.

(26) Irimura, T.; Nakajima, M.; Nicolson, G. L. Chemically modified heparins as inhibitors of heparan sulfate specific endo-beta-glucuronidase (heparanase) of metastatic melanoma cells. *Biochemistry* **1986**, *25*, 5322−8.